Kinetic Aspects of Ethanol Electrooxidation on Catalytic Surfaces of Pt in 0.5 M H$_2$SO$_4$

Boguslaw Pierozynski[*]

Department of Chemistry, Faculty of Environmental Protection and Agriculture, University of Warmia and Mazury in Olsztyn, Plac Lodzki 4, 10-957 Olsztyn, Poland
[*]E-mail: boguslaw.pierozynski@uwm.edu.pl

The present study reports cyclic voltammetric and a.c. impedance spectroscopy investigations of electrooxidation process of ethanol on Pt catalytic surfaces, carried-out in 0.5 M H$_2$SO$_4$ solution. The kinetics of ethanol electrooxidation were examined on polycrystalline Pt, Pt(111) and (100) single-crystal surfaces, also in relation to those of the process of underpotential deposition (UPD) of H at Pt. In reference to the temperature dependence, electrochemical examinations were performed for variable temperature range, from 23 through 60 ^{o}C.

1. INTRODUCTION

Electrochemical oxidation of alcohols has a direct application in the so-called DAFC (*Direct Alcohol Fuel Cell*) devices. While pure hydrogen allows to obtain higher electric efficiency than alcohols in a PEM (*Proton Exchange Membrane*)-based fuel cell, its production, storage and distribution are still not fully structured for a large scale system. On the other hand, the use of alcohols as H carriers in a DAFC device is advantageous, because alcohols are liquids (simplified fuel storage and distribution systems are involved). In addition, alcohols can provide relatively high mass energy-density (e.g. 6.1 and 8.0 kWh kg^{-1} for methanol, and ethanol, respectively) [1-8].

The most widely studied alcohols for PEMFC applications are methanol and ethanol fuels, where the latter one is considered a promising substitute for the former, due to its higher (by *ca.* 30 %) energy-density and non-toxic properties (ethanol oxidation by-products, i.e. acetaldehyde and acetic acid, are significantly less detrimental to health than methanol itself, or its oxidation by-products).

Ethanol is a renewable resource as it can easily be produced from a variety of available agricultural products and biomass substrates [1-3, 8].

The process of electrooxidation of ethanol on a Pt-based catalyst surface is a complex anodic reaction, which involves generation of numerous, surface-adsorbed reaction intermediates. It is generally accepted [2, 9, 10] that following the surface electrosorption step, ethanol molecule can either dissociate to surface-adsorbed CO species or it could become oxidized to form acetaldehyde. Then, in the presence of adsorbed OH, consecutive oxidation steps lead to the formation of CO_2 or acetic acid, following their desorption from the catalyst surface. A large number of catalytic materials, including bulk polycrystalline [3] and various single-crystal planes of Pt [3, 10-12], PtRu [2, 13], PtRh [2, 9], PtSn [1, 2, 6, 7, 12, 14] and PtPd [8] alloys/co-deposits (typically on carbon substrate) have extensively been examined towards their electrochemical behaviour for ethanol oxidation. However, development of efficient (and price-competitive) anode electrocatalyst material for DEFC systems still presents a difficult challenge.

This work constitutes a comprehensive electrochemical study of the process of ethanol oxidation on the selected Pt catalytic materials, namely: polycrystalline Pt, Pt(111) and (100) single-crystals in 0.5 M H_2SO_4 solution. Most importantly, kinetic characteristics of this process in relation to the kinetics of the process of underpotential deposition of H at Pt, and in function of changing temperature, have been addressed in detail.

2. EXPERIMENTAL

2.1. Solutions and solutes

High-purity solutions were prepared from water derived from an 18.2 MΩ Direct- Q3 UV ultra-pure water purification system from Millipore. Aqueous 0.5 M H_2SO_4 solution was made up from sulphuric acid of highest purity available (SEASTAR Chemicals, BC, Canada). Ethanol (Stanlab, pure, p.a., Poland) was used to prepare acidic solutions, at concentrations of 0.25 and 1.0 M C_2H_5OH. Before conducting experiments, all solutions were de-aerated with high-purity argon (Ar 6.0 grade, Linde), the flow of which was also maintained above the solutions during the cyclic voltammetry and impedance spectroscopy measurements.

2.2. Electrochemical cell, reference and counter electrodes

An electrochemical cell, made all of Pyrex glass, was used during the course of this work. The cell comprised three electrodes: a Pt-based working electrode (WE), equipped with flexible adjustment (in a central part), a reversible Pd hydrogen electrode (RHE) as reference and a Pt counter electrode (CE), both in separate compartments. Special care was taken to minimize the ohmic resistance (IR) drop by locating the Luggin capillary at the centre of the cell. Also, a 0.5 mm diameter Pt wire was installed between and within the tip of the Luggin capillary and the RHE reference compartment. This arrangement (allowing for significant elimination of the IR potential drop) was essential for the fast responses required for a.c. impedance spectroscopy. Prior to each series of experiments, the

electrochemical cell was taken apart and soaked in hot sulphuric acid for at least 3 hours. After having been cooled to about 40 ^{o}C, the cell was thoroughly rinsed with Millipore ultra-pure water. An identical procedure was applied for cleaning all the glassware used to prepare supporting electrolyte.

The palladium hydrogen electrode, acting as a reversible hydrogen electrode (RHE) was used throughout this work. Hence, all the potentials are given on the RHE scale. The palladium RHE was made of a coiled Pd wire (0.5 mm diameter, 99.9 % purity, Aldrich) and sealed in soft glass. Before its use, this electrode was cleaned in hot sulphuric acid, followed by cathodic charging with hydrogen in 0.5 M H_2SO_4 (at current, I_c= 10 mA), until H_2 bubbles in the electrolyte were clearly observed. A counter electrode was made of a coiled Pt wire (1.0 mm diameter, 99.9998 % purity, Johnson Matthey, Inc.). Prior to its use, the counter electrode was either cleaned in hot sulphuric acid or was flame-annealed.

2.3. Equipment and Pt-based catalyst materials

Cyclic voltammograms were recorded at 296 K (room temperature: 23 ^{o}C) and over the temperature range: 23 through 60 ^{o}C (for the temperature-dependent experiments), at a sweep-rate of 50 mV s^{-1} by means of the *Solartron* 12,608 W Full Electrochemical System, consisting of 1260 frequency response analyzer (FRA) and 1287 electrochemical interface (EI). For a.c. impedance measurements (carried-out over the temperature range: 23-60 ^{o}C), the 1260 FRA generator provided an output signal of known amplitude (5 mV) and the frequency range was typically swept between 1.0×10^5 and 0.5×10^{-1} Hz. The instruments were controlled by *ZPlot 2.9* or *Corrware 2.9* software for Windows (Scribner Associates, Inc.). Presented here impedance results were obtained through selection and analysis of representative series of experimental data. Typically, three impedance measurements were conducted at each potential value. Reproducibility of such-obtained results was usually below 10 % from one measurement to another. The impedance data analysis was performed with *ZView 2.9* software package, where the spectra were fitted by means of a complex, non-linear, least-squares immitance fitting program, *LEVM 6*, written by Macdonald [15]. Three equivalent circuits for identified charge-transfer surface processes, including constant-phase elements (CPEs) to account for distributed capacitance were employed to analyze the obtained impedance results, as later shown in Figs. 5a through 5c below.

Polycrystalline Pt and Pt single-crystals of the (111) and (100) orientations were made from 1 mm diameter 99.9985 % Pt wire (AESAR/Puratronic). Single-crystal electrodes were prepared by employing the techniques and procedures for preparation of Pt single-crystals, developed by Clavilier et al. [16-19], where the crystals' orientations were determined by means of the back von Laue X-ray diffraction method [20, 21].

3. RESULTS AND DISCUSSION

3.1. Electrooxidation of ethanol by cyclic voltammetry

The cyclic voltammetric behaviour of the process of electrooxidation of ethanol on polycrystalline Pt electrode surface in 0.5 M H_2SO_4 is shown in Fig. 1 below. Hence, two oxidation

peaks, centred at *ca*. 0.80 and 1.30 V vs. RHE appear upon an anodic sweep in Fig. 1. Then, when the CV sweep is reversed towards the H_2 reversible potential, a single anodic peak is revealed and centred at *ca*. 0.65 V. Electrooxidation process follows a surface adsorption step of ethanol molecules, which likely takes place over the potential range *ca*. 0.20-0.40 V, partly in parallel with UPD H ionization from the Pt surface.
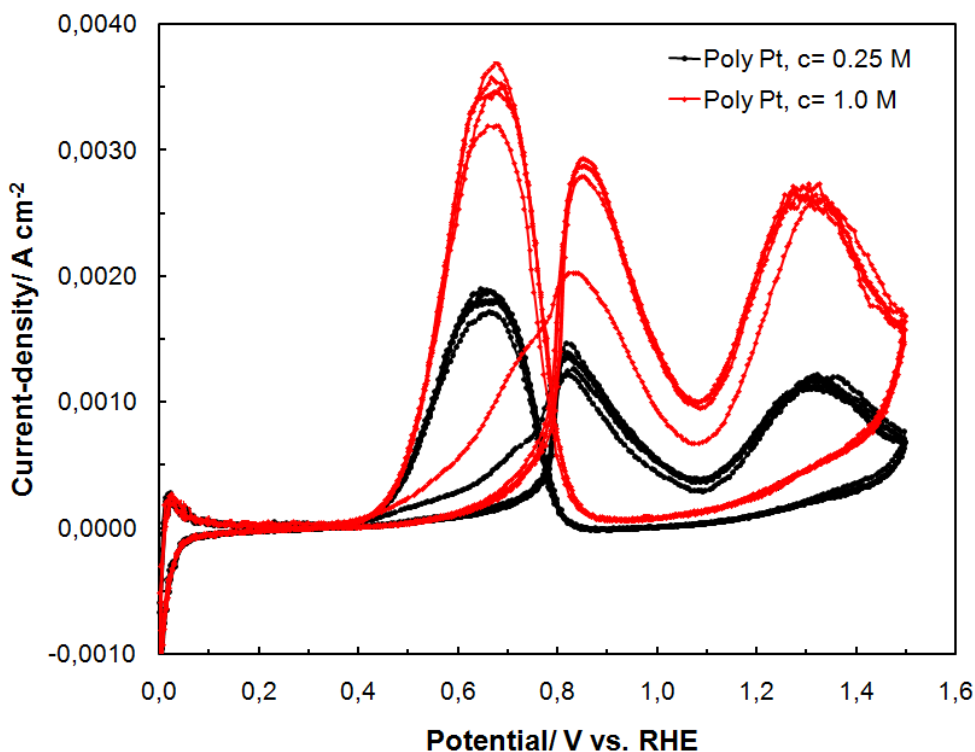
Figure 1. Cyclic voltammograms for ethanol electrooxidation on polycrystalline Pt electrode, carried-out in 0.5 M H_2SO_4, at a sweep-rate of 50 mV s^{-1} and in the presence of 0.25, and 1.0 M C_2H_5OH (five consecutive cycles were recorded for each CV run).

The lowest potential oxidation peak (0.65 V) is generally attributed in relevant literature to the process of oxidation of surface-adsorbed CO_{ads} species, while that at 0.80 V to the formation of acetaldehyde [3, 10, 11]. In contrast, the third, high potential anodic peak (*ca*. 1.10-1.50 V), very likely refers to the oxidation process, with active involvement of surface-adsorbed, oxygen-like species. Furthermore, increased concentration of ethanol (from 0.25 to 1.0 M C_2H_5OH) resulted in a radical magnification of the current-density for all oxidation peaks, as observed in the corresponding voltammetric profile in Fig. 1.

On the other hand, significantly increased catalytic activity was observed for Pt(111) and (100) single-crystals, especially for the (100) plane (see Fig. 2), where under similar experimental conditions (at 0.25 M C_2H_5OH), the recorded maximum current-density at *ca*. 0.80 V was about 7 times as high as the current-density value at the corresponding potential for the polycrystalline Pt electrode in Fig. 1.
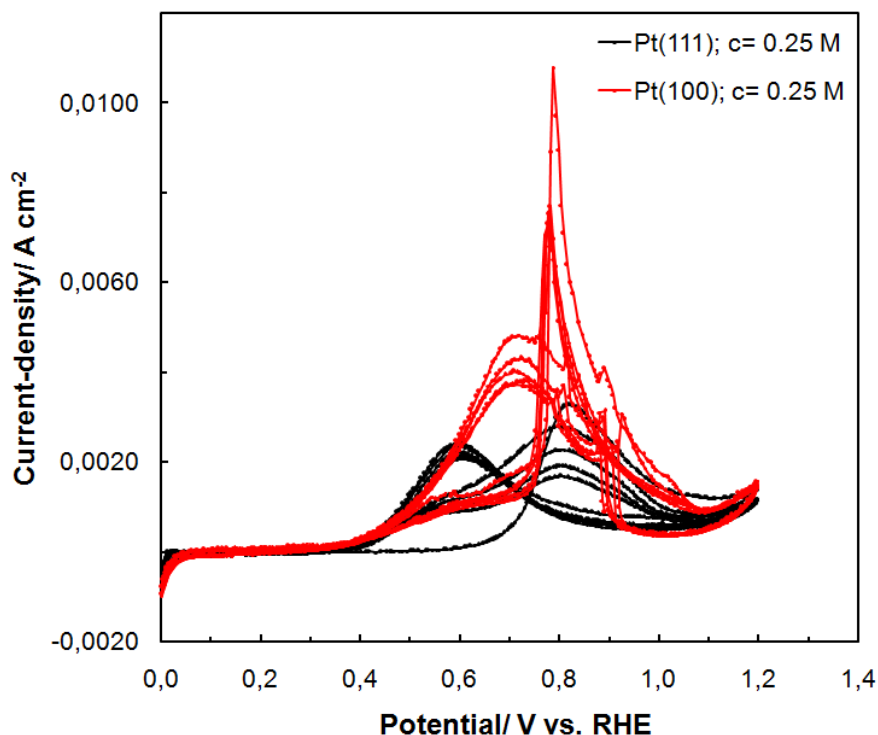
Figure 2. Cyclic voltammograms for ethanol electrooxidation on Pt(111) and (100) single-crystal surfaces, carried-out in 0.5 M H$_2$SO$_4$, at a sweep-rate of 50 mV s^{-1} and in the presence of 0.25 M C$_2$H$_5$OH (five consecutive cycles were recorded for each CV run).

*3.2. Electrooxidation of ethanol by a.c. impedance spectroscopy*

Table 1. Resistance and capacitance parameters for electrooxidation of ethanol (at 0.25 and 1.0 M C$_2$H$_5$OH) and UPD of H on polycrystalline Pt electrode in 0.5 M H$_2$SO$_4$ (at 296 K), obtained by finding the equivalent circuits which best fitted the impedance data, as shown in Figs. 5a[a] and 5b[b].

E/ mV	R$_H$/ Ω cm^2	x10^6 C$_{pH}$/ F cm^{-2}s$^{\varphi 1-1}$	x10^6 C$_{dl}$/ F cm^{-2}s$^{\varphi 2-1}$	R$_{ct}$/ Ω cm^2
0.25 M C$_2$H$_5$OH				
200[a]	55.8 ± 4.5	67.2 ± 7.2	63.3 ± 7.7	105,793 ± 13,800
250[a]	183.1 ± 5.6	38.1 ± 1.1	27.2 ± 0.9	53,748 ± 1,967
300[a]	753.4 ± 37.6	7.8 ± 0.3	18.8 ± 0.3	47,898 ± 594
400[b]	-----	-----	18.9 ± 0.1	25,477 ± 232
500[b]	-----	-----	23.8 ± 0.3	4,051 ± 54
600[b]	-----	-----	54.7 ± 1.2	1,920 ± 31
1.0 M C$_2$H$_5$OH				
200[a]	73.5 ± 3.4	62.8 ± 3.3	43.7 ± 3.4	57,814 ± 5,723
250[a]	288.9 ± 8.4	23.9 ± 0.6	21.4 ± 0.5	47,186 ± 1,321
400[b]	-----	-----	15.6 ± 0.1	24,103 ± 205
500[b]	-----	-----	17.1 ± 0.2	3,596 ± 30
600[b]	-----	-----	40.9 ± 1.6	782 ± 14

The a.c. impedance characteristics of the process of electrooxidation of ethanol (in the presence of UPD of H) on the three selected Pt catalyst materials in 0.5 M H_2SO_4 are presented in Tables 1 and 2, and in Figs. 3 and 4 below.
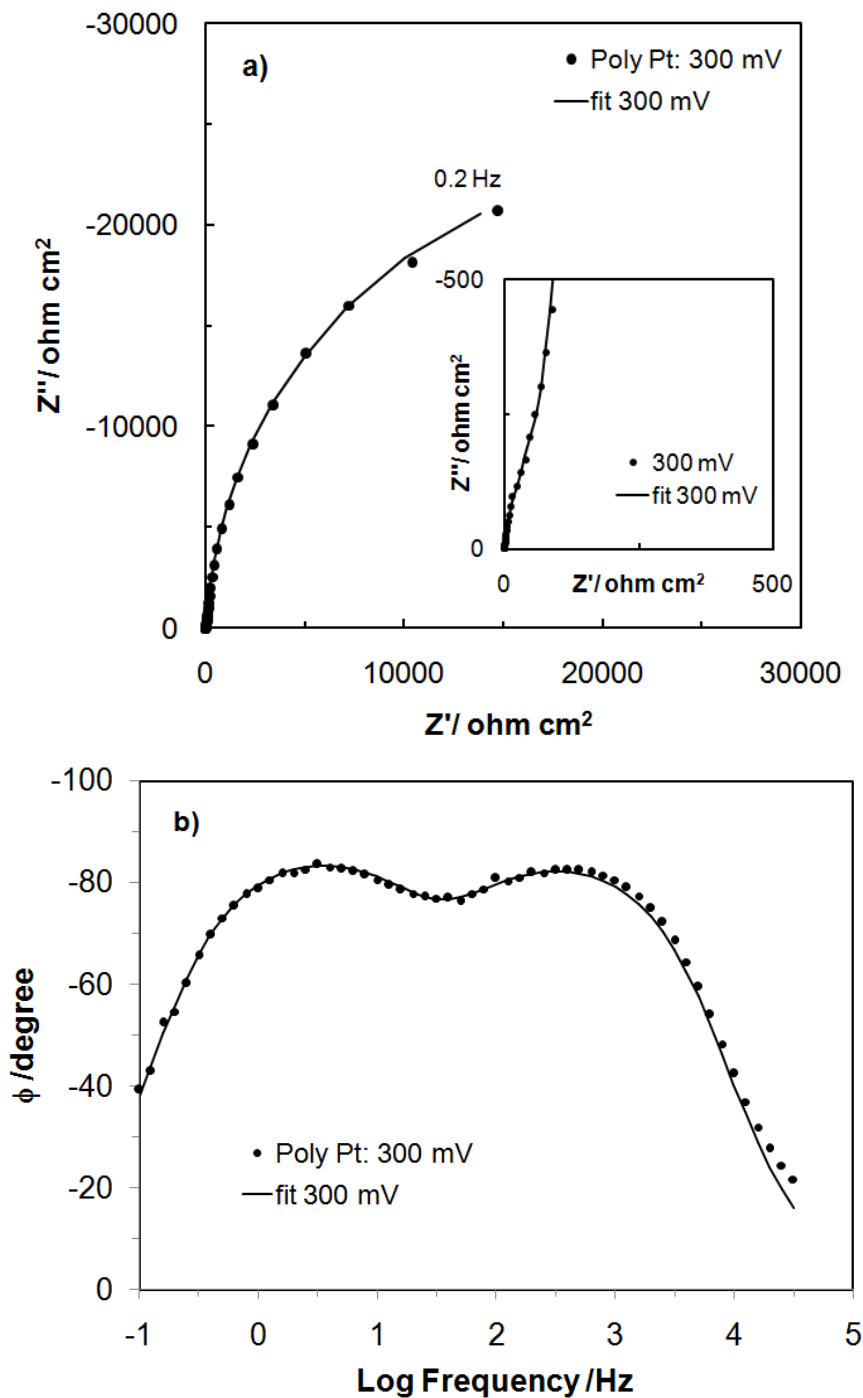
Figure 3. a) Complex-plane impedance plot for polycrystalline Pt in contact with 0.5 M H_2SO_4, in the presence of 0.25 M C_2H_5OH, recorded at 300 mV vs. RHE (at 296 K). The solid line corresponds to representation of the data according to the equivalent circuit shown in Fig. 5a; b) Bode phase-angle plot showing 2 maxima, observed over high and low frequency regions, respectively (other details as in Fig. 3a above).
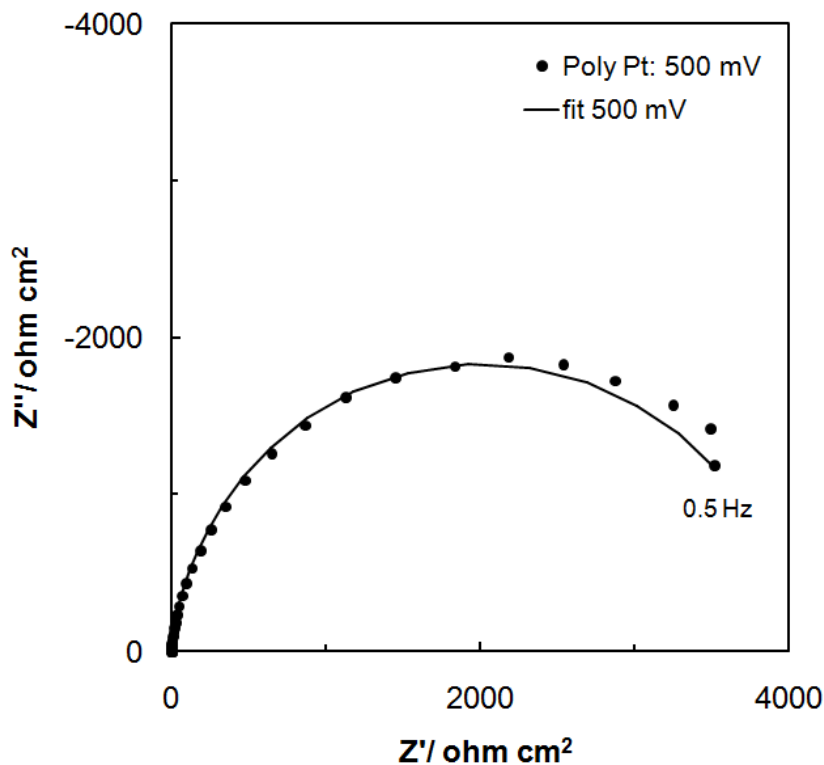
Figure 4. Complex-plane impedance plot for polycrystalline Pt in contact with 0.5 M H_2SO_4, in the presence of 0.25 M C_2H_5OH, recorded at 500 mV vs. RHE (at 296 K). The solid line corresponds to representation of the data according to the equivalent circuit shown in Fig. 5b.

Hence, for the polycrystalline Pt electrode, the onset of ethanol oxidation (at 0.25 M C_2H_5OH) can already be observed for the potential range: 200-300 mV vs. RHE, i.e. over the potential range characteristic to UPD of H (see Table 1). The recorded values of the charge-transfer resistance parameter (R_H) for the process of UPD of H are dramatically increased (*ca.* 2-3 orders in magnitude), as compared to those previously reported in literature for Pt single-crystal planes in 0.5 M sulphuric acid [22, 23]. Extremely high values of the R_H resistance coincide with very low adsorption pseudocapacitance (C_{pH}) values (67 and 8 μF $cm^{-2}s^{\varphi 1-1}$ were recorded at 200, and 300 mV, correspondingly, see Table 1). The above is very likely the result of strong interference from the adsorption of ethanol molecules, taking place over the potential range for underpotential, reversible deposition of H on Pt (*ca.* 100-400 mV vs. RHE). Here, for the potential range: 200-300 mV, the Nyquist impedance spectra exhibit two partial, somewhat distorted semicircles (see Fig. 3a as an example of electrochemical behaviour at 300 mV). The smaller partial semicircle (see inset to Fig. 3a), observed only at high frequencies, corresponds to the process of UPD of H, and a large-diameter semicircle, observed throughout the intermediate frequency range, is associated with the charge-transfer process (R_{ct}) accompanying ethanol electrooxidation on the Pt surface. In addition, existence of two maxima can clearly be detected in the corresponding Bode phase-angle plot in Fig. 3b.

Then, over the potential range: 400-600 mV, a single partial semicircle (related to the process of ethanol electrooxidation) appears in the Nyquist impedance plot (see as an example Fig. 4 above). Minimum of the charge-transfer resistance parameter (R_{ct} = 1,920 Ω cm^2) for ethanol oxidation was

recorded at 600 mV, which is near the peak current-density potential value in Fig. 1. Furthermore, increased alcohol concentration (from 0.25 to 1.0 M C_2H_5OH) significantly facilitated the kinetics of the oxidation process, leading (comparatively) to reduction of the minimum value of the R_{ct} parameter (at 600 mV) by *ca.* 2.5 times (Table 1). However, higher concentration of ethanol also caused a dramatic increase of the charge-transfer resistance parameter for the process of UPD of H (e.g. compare the recorded R_H values of *ca.* 183 and 289 Ω cm^2 at 250 mV for C_2H_5OH concentrations of 0.25 and 1.0 M, correspondingly).
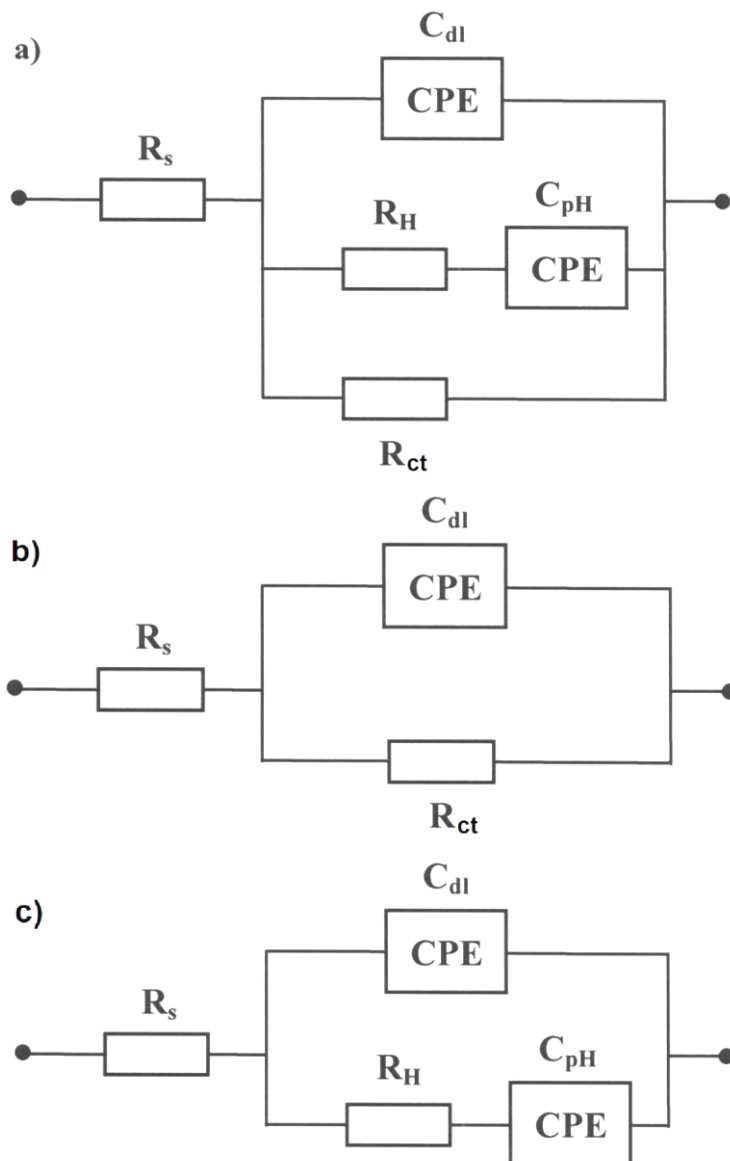
Figure 5. Three equivalent circuits, used for fitting the obtained a.c. impedance spectroscopy data in this work, where: R_s is solution resistance, C_{dl} is double-layer capacitance, R_H and C_{pH} are resistance and pseudocapacitance parameters for the process of UPD of H, R_{ct} is charge-transfer resistance parameter for electrooxidation of ethanol. The circuits include two constant phase elements (CPEs) to account for distributed capacitance.

On the other hand, the double-layer capacitance values, C_{dl}, showed significant fluctuations (from below 20 to *ca*. 63 μF cm^{-2}s$^{\varphi2-1}$). Considerably increased C_{dl} (above that commonly used value of 20 μF cm^{-2} in literature for smooth and homogeneous surfaces [24, 25]) implies considerable contribution from surface adsorption processes that might take place over the corresponding potential range. Furthermore, a deviation from the purely capacitive behaviour (which demanded the use of the CPE components in the equivalent circuits, see Figs. 5a through 5c) corresponds to distribution (dispersion) of capacitance. This effect is typically assigned to slow ion adsorption-desorption processes (as previously suggested by Pajkossy [26]) or to increasing surface inhomogeneity, being a possible result of prolonged potentiostatic impedance measurements [26-28]. In this work, values of dimensionless parameters φ_1 and φ_2 (for the CPE components) oscillated between 0.86 and 0.98. Please note that $0 \leq \varphi \leq 1$ and when $\varphi=1$, the CPE acts just like a pure capacitor.

Table 2. Resistance and capacitance parameters for electrooxidation of ethanol (at 0.25 M C_2H_5OH) and UPD of H on Pt(111) and (100) electrode surfaces in 0.5 M H_2SO_4 (at 296 K), obtained by finding the equivalent circuits which best fitted the impedance data, as shown in Figs. 5b[b] and 5c[c].

E/ mV	R_H/ Ω cm^2	x10^6 C_{pH}/ F cm^{-2}s$^{\varphi1-1}$	x10^6 C_{dl}/ F cm^{-2}s$^{\varphi2-1}$	R_{ct}/ Ω cm^2
Pt (111)				
500[b]	-----	-----	15.1 ± 0.2	12,101 ± 632
600[b]	-----	-----	22.3 ± 0.3	2,865 ± 27
700[b]	-----	-----	27.1 ± 0.8	883 ± 11
Pt (100)				
200[c]	4.8 ± 0.1	389.9 ± 7.6	59.6 ± 7.1	-----
300[c]	88.9 ± 3.0	42.2 ± 1.3	28.1 ± 1.0	-----
400[b]	-----	-----	19.1 ± 0.2	23,840 ± 1,302
500[b]	-----	-----	19.4 ± 0.2	6,844 ± 116
600[b]	-----	-----	65.3 ± 0.9	2,475 ± 44
700[b]	-----	-----	79.2 ± 4.1	80.4 ± 2.7

Employment of Pt single-crystal electrodes led to significant facilitation of the process of ethanol electrooxidation. Thus, for the Pt(111) plane, the minimum charge-transfer resistance value of 883 Ω cm^2 (for 0.25 M C_2H_5OH) was recorded at the potential of 700 mV (see Table 2). Please note however that the rates for UPD of H on this Pt plane were not accessible under the experimental conditions (compare with the corresponding conclusions of Morin et al. given in Ref. 22). For this reason, for potentials below 500 mV vs. RHE, only purely capacitive impedance behaviour (with some CPE effect) was observable in the complex-plane impedance plots on the Pt(111) surface. Conversely, electrooxidation of ethanol becomes dramatically enhanced on the surface of the Pt(100) electrode. Here, minimum of the respective R_{ct} parameter comes to 80.4 Ω cm^2 at 700 mV (also refer to the relevant CV profile in Fig. 2), which corresponds to 11-fold reduction of the charge-transfer resistance [compared to the (111) case]. In addition, the rates for UPD of H on the (100) plane become

dramatically inhibited by the main, ethanol surface electro-sorption(oxidation) process. In fact, the recorded values of the R_H parameter in Table 2 (for the potential range: 200-300 mV) are about 12x (at 200 mV) and 340x (at 300 mV) as high as those recently recorded for Pt(100) in pure 0.5 M H_2SO_4 in Ref. 23. In this respect, the kinetics of the process of UPD of H at the Pt(100) plane are fairly consistent with those recorded for the polycrystalline Pt electrode in Table 1. Again, the recorded in Table 2 double-layer capacitance values oscillated between *ca.* 15 and 79 $\mu F\ cm^{-2}s^{\varphi2-1}$, whereas those of the dimensionless parameters (φ_1 and φ_2) were between 0.89 and 0.98.

3.3. Electrooxidation of ethanol: temperature-dependence for polycrystalline Pt
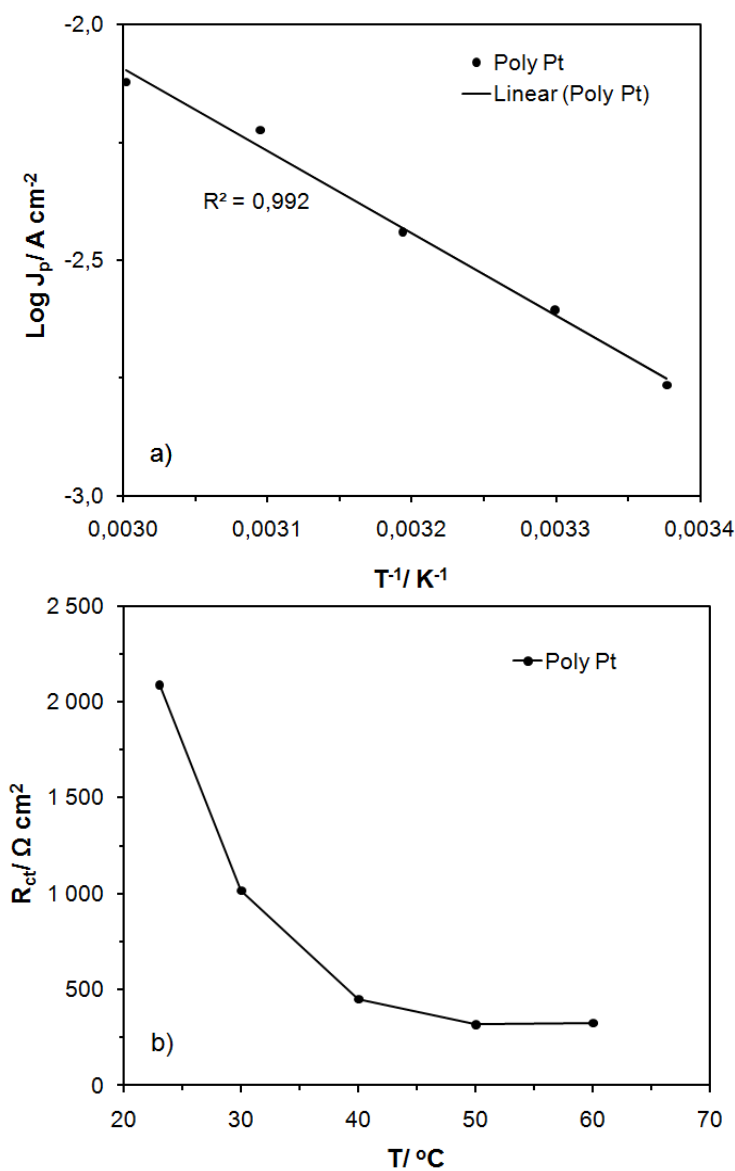
Figure 6. a) Arrhenius plot for ethanol electrooxidation (at 0.25 M C_2H_5OH) on polycrystalline Pt electrode in contact with 0.5 M H_2SO_4, recorded for the anodic peak current-density value; b) Variation of charge-transfer resistance, R_{ct} parameter, for ethanol electrooxidation (at 0.25 M C_2H_5OH) with temperature for polycrystalline Pt electrode in contact with 0.5 M H_2SO_4, recorded at 700 mV vs. RHE.

The process of electrooxidation of ethanol exhibited considerable temperature-dependence. Fig. 6a above presents an Arrhenius plot for ethanol oxidation (at 0.25 M C_2H_5OH) on the polycrystalline Pt electrode, recorded for the peak anodic current-density value (refer to Fig. 1), over the temperature range: 23-60 °C. Thus, augmentation of the reaction temperature led to a significant increase of the recorded voltammetric oxidation current-densities. The above can be supported by a strong, temperature dependence of the charge-transfer resistance, R_{ct} parameter, as shown in Fig. 6b (please note that an appropriate correction was introduced [29], in order to account for a small, but significant temperature shift of the Pd RHE over the studied temperature range).

The Arrhenius plot-derived apparent activation energy (E_A) for electrooxidation of ethanol on polycrystalline Pt came to 33.4 kJ mol^{-1}. The above obtained value is in fairly good agreement with those recorded for various Pt-based catalyst materials in relevant literature [6, 8, 9].

4. CONCLUSIONS

The process of electrooxidation of ethanol (carried-out in H_2SO_4 supporting electrolyte) proved to be highly specific to geometry of Pt single-crystal catalysts, where Pt(100) plane exhibited significantly enhanced catalytic properties towards ethanol oxidation, as compared to those demonstrated by Pt(111) surface or a polycrystalline Pt electrode. The onset of ethanol electrooxidation extends over the potential range characteristic to the reversible deposition (UPD) of H on Pt. The presence of ethanol molecules (or reaction intermediates) on the surface of Pt catalyst dramatically affects the rates for UPD of H (slowing them down by several orders in magnitude), as compared to those obtained in the absence of ethanol in the supporting electrolyte. Kinetics of ethanol electrooxidation on the Pt catalyst material are found strongly dependent on the reaction temperature, as well as on the concentration of ethanol in the electrolyte.

References

1. S. Rousseau, C. Coutanceau, C. Lamy and J.M. Leger, *J. Power Sources*, 158 (2006) 18.
2. S.Q. Song, W.J. Zhou, Z.H. Zhou, L.H. Jiang, G.Q. Sun, Q. Xin, V. Leontidis, S. Kontou and P. Tsiakaras, *Int. J. Hydrogen Energy*, 30 (2005) 995.
3. A.A. Abd-El-Latif, E. Mostafa, S. Huxter, G. Attard and H. Baltruschat, *Electrochim. Acta*, 55 (2010) 7951.
4. S.B. Han, Y.J. Song, J.M. Lee, J.Y. Kim and K.W. Park, *Electrochem. Commun.*, 10 (2008) 1044.
5. M.H. Shao and R.R. Adzic, *Electrochim. Acta*, 50 (2005) 2415.
6. S.S. Gupta, S. Singh and J. Datta, *Mat. Chem. Phys.*, 120 (2010) 682.
7. E.E. Switzer, T.S. Olson, A.K. Datye, P. Atanassov, M.R. Hibbs and C.J. Cornelius, *Electrochim.*

Acta, 54 (2009) 989.

8. S.S. Mahapatra, A. Dutta and J. Datta, *Electrochim. Acta*, 55 (2010) 9097.
9. S.S. Gupta and J. Datta, *J. Electroanal. Chem.*, 594 (2006) 65.
10. X.H. Xia, H.D. Liess and T. Iwasita, *J. Electroanal. Chem.*, 437 (1997) 233.
11. J.F. Gomes, B. Busson, A. Tadjeddine and G. Tremiliosi-Filho, *Electrochim. Acta*, 53 (2008) 6899.
12. A.A. El-Shafei and M. Eiswirth, *Surf. Sci.*, 604 (2010) 862.
13. N. Fujiwara, Z. Siroma, S. Yamazaki, T. Ioroi, H. Senoh and K. Yasuda, *J. Power Sources*, 185 (2008) 621.
14. F.C. Simoes, D.M. dos Ajnos, F. Vigier, J.M. Leger, F. Hahn, C. Coutanceau, E.R. Gonzalez, G. Tremiliosi-Filho, A.R. de Andrade, P. Olivi and K.B. Kokoh, *J. Power Sources*, 167 (2007) 1.
15. J. R. Macdonald, *Impedance Spectroscopy, Emphasizing Solid Materials and Systems*, John Wiley & Sons, Inc., New York, (1987).
16. J. Clavilier and R. Pineaux, *C.R. Acad. Sci. Paris*, 260 (1965) 891.
17. J. Clavilier, *J. Electroanal. Chem.*, 107 (1980) 211.
18. J. Clavilier, R. Faure, D. Guinet and R. Durand, *J. Electroanal. Chem.*, 107 (1980) 205.
19. J. Clavilier, K. El Achi, M. Petit, A. Rodes and M.A. Zamakhchari, *J. Electroanal. Chem.*, 295 (1990) 333.
20. C.S. Barret and T.B. Massalski, *"Structure of Metals: Crystallographic Methods, Principles and Data"*, McGraw Hill, London, (1966).
21. A. Hamelin in "*Modern Aspects of Electrochemistry"*, B.E. Conway, J.O'M. Bockris and R.E. White (Eds.), Plenum Press, New York, 1 (1985) 16.
22. S. Morin, H. Dumont and B.E. Conway, *J. Electroanal. Chem.*, 412 (1996) 39.
23. B.E. Conway and B. Pierozynski, *J. Electroanal. Chem.*, 622 (2008) 10.
24. A. Lasia and A. Rami, *J. Applied Electrochem.*, 22 (1992) 376.
25. L. Chen and A. Lasia, *J. Electrochem. Soc.*, 138 (1991) 3321.
26. T. Pajkossy, *J. Electroanal. Chem.*, 364 (1994) 111.
27. B.E. Conway in *Impedance Spectroscopy. Theory, Experiment, and Applications*, E. Barsoukov and J. Ross Macdonald (Eds.), Wiley-Interscience, John Wiley & Sons, Inc., Hoboken, N.J., 4.5.3.8 (2005) 494.
28. W.G. Pell, A. Zolfaghari and B.E. Conway, *J. Electroanal. Chem.*, 532 (2002) 13.
29. A. Prokopowicz and M. Opallo, *Solid State Ionics*, 157 (2003) 209.